Terrain Moisture and stream Level for Integrated Reflected GPS System using Reflectivity and Elevation Map

Lie Chung Shen
Department of Earth Science, NCKU ;Taiwan (E-mail: shens.art@msa.hinet.net)
Jyh Ching Juang
Department of Electric Engineering, NCKU , Taiwan (E-mail:juang@mail.ncku.edu.tw)
Char Chang Chang
Department of Applied Geometric, Ching -Yun University, Taiwan (E-mail: ccchang50@cyu.edu.tw)

Abstract: This paper reports on work that demonstrates terrain moisture and stream level by using integrated reflected GPS system. The goal of this study is to exploit the carrier phase, Doppler shift, reflectivity of L1/L2 signal-to-noise density ratio components of the reflected signals and direct signals for stream water and ground object detection with surface. The altitude accuracy of the system was improved from 5.5 to 3.5 m (RMS) for Integrated Reflected GPS System within undulation height module and from 3.5 to 1.1 m (RMS) for the Reflected GPS System using Digital Terrain Evaluation Data (DTED) Map system. The each instantaneous moving surface should be exploited by each reflected GPS carrier phase and reflected point. For remote sensing of stream, ocean, and landscape, the accuracies of each reflected altitude are among 10 cm and 30 cm. A field test has been conducted and the results indicate that the stream surface currents are predicted by using GPS Doppler shifts due to surface reflection as a moving surface. The stream surface currents are estimated to be around 0.1–7.0 m/s by using Doppler shifts and derived from water level module. The classification accuracies was improved about 55 -65 % by using the multi-spectral (green, red, blue and reflectivity) data coupled with rough surfaces parameters at terrain soil moisture was improved by using correction factor. This GPS reflectivity of stream, stream soil moisture, coastal soil moisture and sea state measurement will provide for a lower cost, high resolution and better accuracy than other land cover, coastal sea state measurements such as airplane and ground based experiments.

Key Words:
1. GPS. 2. Doppler shifts. 3. Rough surfaces. 4. Reflectivity. 5. Remote sensing. 6. Soil moisture.

1. INTRODUCTION A reflected GPS signal contains information on the reflecting object since the characteristics of the reflected signal vary considerably depending on the reflecting object [1]. This information pertaining to ground object detection may be useful for the computation of the accurate position of the object with terrain multipath, which is modeled with digital elevation models (DEMs) that are accurate to within ~20 cm [2]. The terrain moisture classes are defined by using two GPS-derived reflectivity classification features and a visual element terrain with land-cover classes containing a surface/soil moisture component [3], [10]. In this study, our objective is to determine the reflectivity of rivers and riverbeds with a rough surface and soil moisture, respectively, by using observations of the GPS L1 (1575.42 MHz) and L2 (1227.60 MHz) frequencies that are received with a highly integrated GPS receiver. Both right-hand circular polarization (*RHCP*) and left-hand circular polarization (*LHCP*) antennas are employed for monitoring river water levels and riverbeds so that the direct and reflected signals can be simultaneously obtained for studying the soil moisture. The direction of arrival of the signals may be that of the reflected signal or the line-of-sight of a particular satellite. The objective of this study is to use the reflectivity of L1 & L2 signal-to-noise density ratio (SNR) components of the reflected signals and direct signals for the detection of flood water levels and soil moisture of riverbeds. An integer ambiguity algorithm has also been implemented for accuracy positions on RHCP and LHCP antenna by using the carrier phase, ionospheric and tropospheric delay of L1 & L2 of the direct signals and reflected signals. The accuracy of the river surface height depends on the heights of the RHCP antenna (used like a base station) and LHCP antenna (used like a mobile receiver). The reflection heights of this system are accurate to within 29 cm ~ 31 cm. The accuracy of the river surface position is determined by a propagation angle model, satellite, RHCP antenna and LHCP antenna positions. The reflection positions of this system are accurate to within 1.1 m ~ 1.25 m. During the development and test stage, the satellite's images are used and mapped with the integrated software for ground object detection.

This paper is structured as follows. At the outset, the reflected positions, reflectivity and surface roughness determined by ground height estimated methods are presented. In section III, the monitoring of flood water levels and soil moisture of riverbeds on the basis of their reflectivity and a ground height estimation method are briefly outlined. Finally, conclusions are drawn from the agreement between theory and the experiments expounded in this paper.

II. MATERIAL AND METHODS

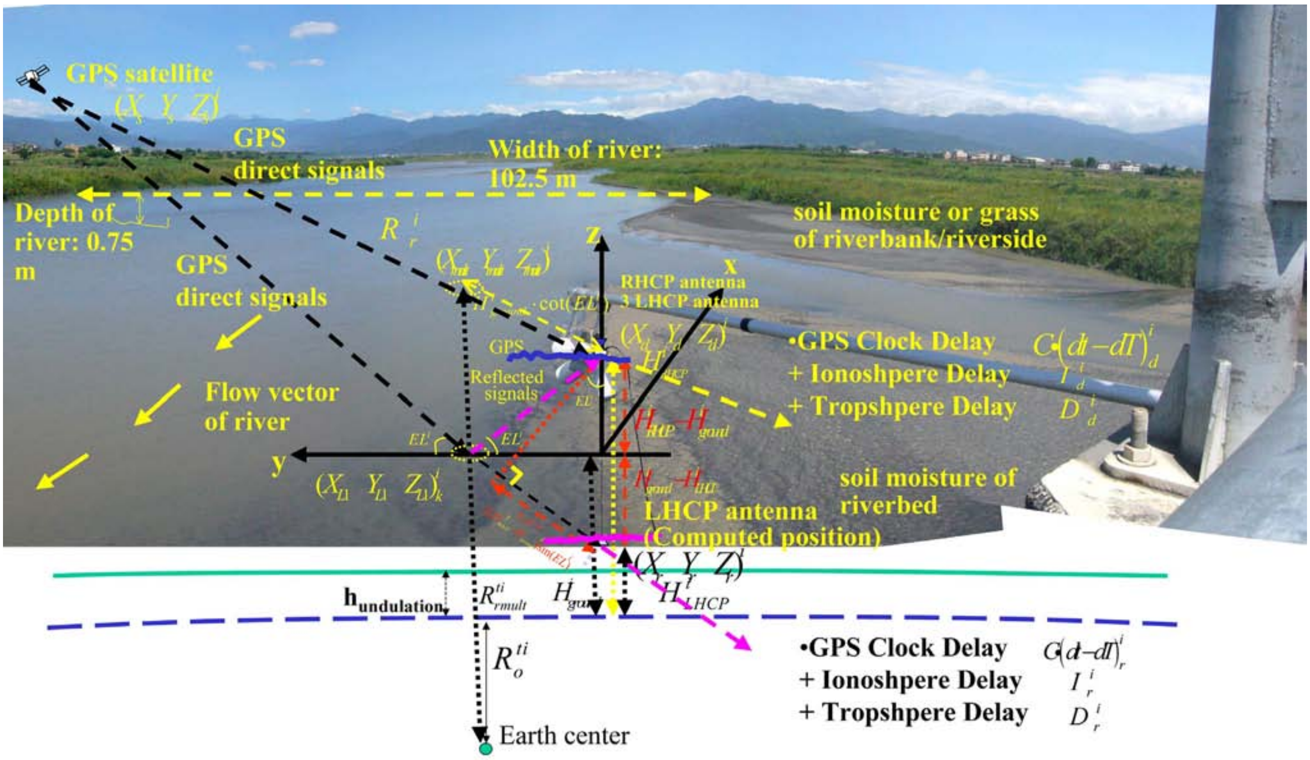

Fig 1

2.1 Basic Principles

The integrated GPS instrument is mounted on a 6.5-m steel pipe containing one RHCP and three LHCP antennas by using two SOKKIA 2600 GPS L1/L2 band receivers. The height of the bridge is 10.5 m (from the bridge floor to the bridge pier). The altitude of the bridge floor is 11.25 m with regard to the ground sea level (shown in Fig. 1). The reflected ray is treated for enhancing its intensity [3], [6]: An N-P connector was used to combine the reflected signals, and the three LHCP antennas (Type: H601; Dbic: 9 dB Hz) are connected to one receiver's RF P-N connector and the RHCP antenna (Type: NovAtel GPS-700; Dbic: 7 dB Hz) is connected to the other receiver's RF P-N connector. The GPS L1/L2 band receivers are two SOKKIA-2600 receivers (with the same motherboard as that of NovAtel DL-4).

In this measurement connection, the measurement for monitoring stream water level, soil classification of riverbed and ground object detection can be found in a related conference paper [4], [5] and in [12].

The system diagram for the monitoring of rivers and the soil moisture of riverbeds is shown in Fig. 2. The receiver enhances 80% of the receiver tracking capability of reflected signals on floodwater surface

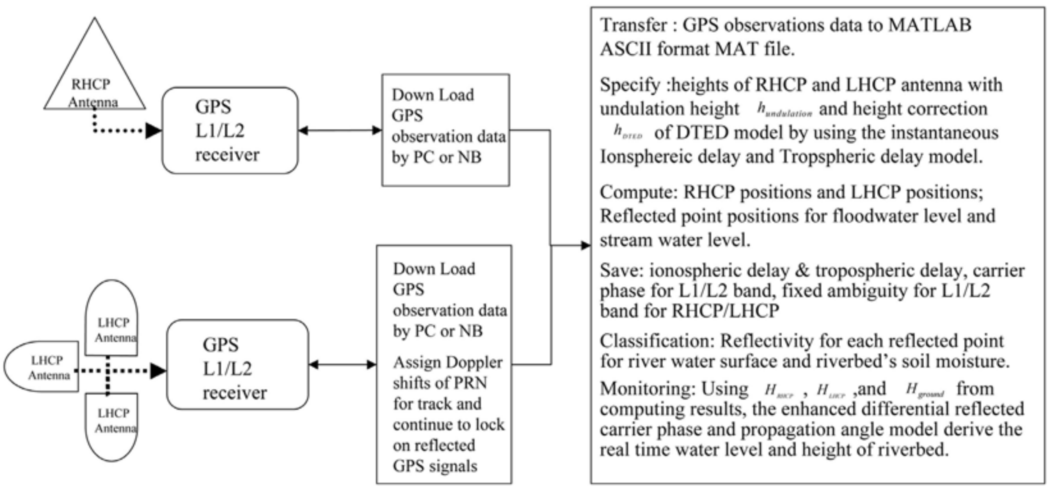

Fig 2

and soil moisture of a riverbed during storm weather.

Let us recall that GPS satellites broadcast signals at L1 and L2 frequencies. Let f_1 and f_2 and λ_1 and λ_2 be the frequencies and wavelengths of L1 and L2, respectively. It is known that dual frequency measurements can be used to effectively remove ionospheric delays. The code and phase measurements at the two frequencies can be expressed as in Goad [7].

$$P_{1s} = R_s + c\left(dt - dT\right)_s - I + D + \varepsilon_{p1s} \tag{1}$$

$$\Phi_{1s} = R_s + c\left(dt - dT\right)_s - I + D + \lambda_1 N_{1s} + \varepsilon_{\phi 1s} \tag{2}$$

$$P_{2s} = R_s + c\left(dt - dT\right)_s + (f_1 / f_2)^2 I + D + \varepsilon_{p2s} \tag{3}$$

$$\Phi_{2s} = R_s + c\left(dt - dT\right)_s - (f_1 / f_2)^2 I + D + \lambda_2 N_{2s} + \varepsilon_{\phi 2s} \tag{4}$$

$$I_s = (f_2^2 / (f_1^2 - f_2^2))\left[\phi_{1s} + \phi_{2s} - (\lambda_1 N_{1s} + \lambda_2 N_{2s}) - (\varepsilon_{\phi 1s} + \varepsilon_{\phi 2s})\right] \tag{5}$$

$$\begin{aligned} D_s = {} & (f_2^2 / (f_1^2 - f_2^2))\left[(\phi_{1s} - \lambda_1 N_{1s} - \varepsilon_{\phi 1s})\right] - \\ & (f_2^2 / (f_1^2 - f_2^2))\left[(\phi_{2s} - \lambda_2 N_{2s} - \varepsilon_{\phi 2s})\right] - (R_s + C(dt - dT))_s \end{aligned} \tag{6}$$

Here, P_{1s} and P_{2s} and Φ_{1s}, and Φ_{2s} are the codes and phases at the L1 and L2 frequencies, respectively. The subscript s is used to represent either the direct (d) signal or the reflected (r) signal. The terms on the right-hand side of (1)–(6) can be explained as follows. R_s is the distance between the satellite and the observation point; $c(dt - dT)_s$, the satellite clock time delay; I_s, the ionospheric delay for the L frequency; D_s, the tropospheric delay; N_{1s}, the integer ambiguity at the L1 frequency; and N_{2s}, the integer ambiguity at the L2 frequency. The remaining terms ε_{p1s}, $\varepsilon_{\phi 1s}$, ε_{p2s}, and $\varepsilon_{\phi 2s}$ represent noise. The procedure for the software simulation processing comprises the following steps.

1. Determination of the antenna position: Typically, a GPS receiver gives an estimate of the position of the antenna in the range of several meters by using P_{1s} CA codes measurements. Using carrier phase measurements and integer ambiguity techniques [8], the position of the antenna can be estimated with an accuracy of several decimeters by using the method of Teunissen [9]. In the software, an altitude iteration loop is also used for further improving the accuracy.
2. Compensation for ionospheric and tropospheric errors: Since dual frequency receivers are used, processing the dual frequency measurements can compensate for ionospheric errors. The tropospheric error is corrected using a tropospheric delay model.
3. Estimation of the reflection point: The reflection point depends on the signal propagation path. As the positions of the antenna and satellite can be computed, the reflection point is constrained to the plane established by the two positions and the geocenter. In the determination of the reflection point, special care is exercised to estimate the altitude as one of the objectives is to estimate the ground object height through the processing of reflected signals. For this estimation, the digital terrain elevation database is used so that the measurements are correlated with the existing model.
4. Estimation of reflectivity: When the attenuated reflected signal is compared with the direct signal, information pertaining to the properties of the ground object is obtained. The signal strengths of the direct and reflected signals are processed to estimate the reflectivity in this step.

In the following, the discussions thus far are briefly summarized using the flow chart in Fig. 3.

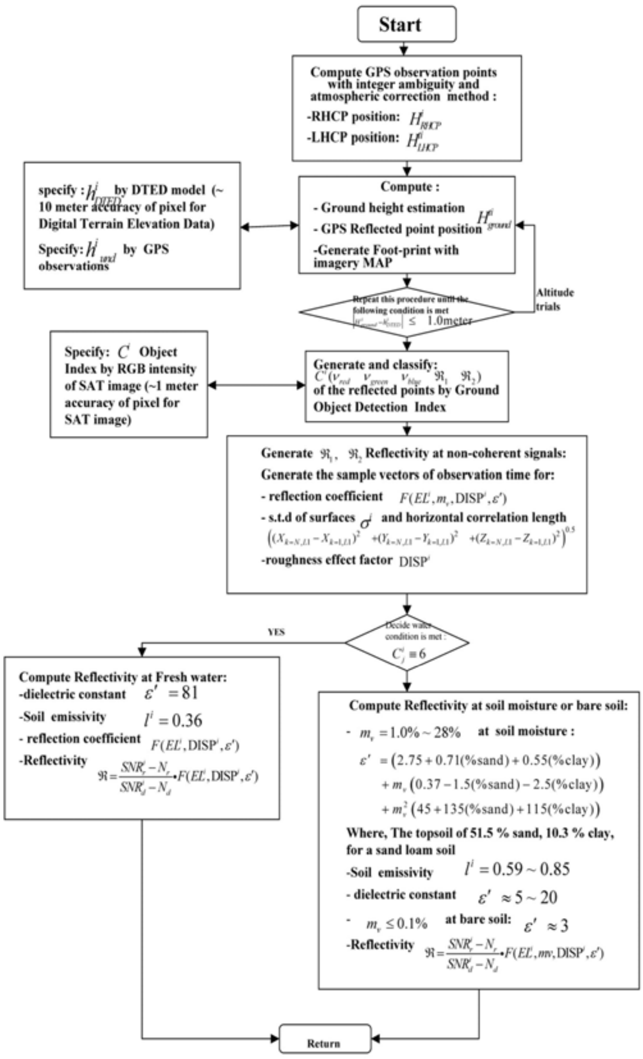

Fig 3

algorithms for the determination of the reflection point, reflectivity, and flood water level are described. Essentially, the reflection point is determined by the propagation angle model on the satellite, RHCP and LHCP positions. The flood water levels are determined by undulation height, RHCP and LHCP heights. In contrast, the reflectivity is estimated by comparing the signal-to-noise ratios between the direct and the reflected signals.

2.2 Ground Height Estimation and Surface Roughness

The RHCP and LHCP fixed positions give different altitudes for the same observation point when the mean of the ground altitude is subject to the estimated ground altitude of the reflected area for each satellite. Then, the altitudes of the RHCP and LHCP positions provide the ground altitude. In Fig. 4., a reflected point on the surface of a flowing stream is shown, and the line of sight between the satellite and the RHCP/LHCP receiver position is observed to be sloping. The RHCP receiver position $(Lon \quad Lat \quad H)_{RHCP}$ is transformed to the $(X_d \quad Y_d \quad Z_d)$ coordinate; the geometry of the line of sight between the receiver position in observation point and five (reflected GPS signals) generators satellites. The reflected receiver position $(Lon \quad Lat \quad H^{ti})_{LHCP}$ is transformed to $(X_r \quad Y_r \quad Z_r)$; ti is the instantaneous number of satellites from which the LHCP receiver receives signals. The satellite position $(Lon \quad Lat \quad H)^i_s$ it is transforms into $(X^i_s \quad Y^i_s \quad Z^i_s)$; i represents the identity of the satellite. The ground or water surface altitude is described by (7) as the project of reflected point on line of sight is $(Lon \quad Lat \quad H)^i_{ground}$ ground transfer to $(X_g \quad Y_g \quad Z_g)^i$; (7) leads to (8). The reflected multi-pole point $(X_{rmult} \quad Y_{rmult} \quad Z_{rmult})^i$ was derived by satellite position with satellite's elevation angle EL^i, R^i_r and RHCP position. R^i_r is the range of RHCP position to satellite position.

$$H^i_{ground} = \frac{(H^i_{RHCP} + H^{ti}_{LHCP})}{2} \tag{7}$$

$$\begin{bmatrix} X_{rmult} \\ Y_{rmult} \\ Z_{rmult} \end{bmatrix}^i = \left[\frac{\left[R^i_r - (H^i_{RHCP} - H^i_{ground}) / \sin\left(EL^i\right) \right]}{R^i_r} \right] * \begin{bmatrix} X_d - X^i_s \\ X_d - X^i_s \\ X_d - X^i_s \end{bmatrix} + \begin{bmatrix} X_s \\ Y_s \\ Z_s \end{bmatrix}^i \tag{8}$$

The (8) and (9) conduct (10) Reflected point center $(X_{L1} \quad Y_{L1} \quad Z_{L1})^i$ as following in:

$$R^i{}_{rmult} = \left\{ \left(X_{rmult}\right)^2 + \left(Y_{rmult}\right)^2 + \left(Z_{rmult}\right)^2 \right\}^{0.5} \tag{9}$$

$$\begin{bmatrix} X_{L1} \\ Y_{L1} \\ Z_{L1} \end{bmatrix}^{ti} = \left[\frac{R^{ti}{}_o + H^i_{ground}}{R^i{}_{rmult}} \right] * \begin{bmatrix} X_{rmult} \\ Y_{rmult} \\ Z_{rmult} \end{bmatrix}^i \tag{10}$$

Where, the value of R^{ti}_o is an ellipsoid radius of the Earth with reference to coordinate (longitude, latitude) of the observation point. The value of R^i_{rmult} is Radius of cross point between Reflected position and line of sight:

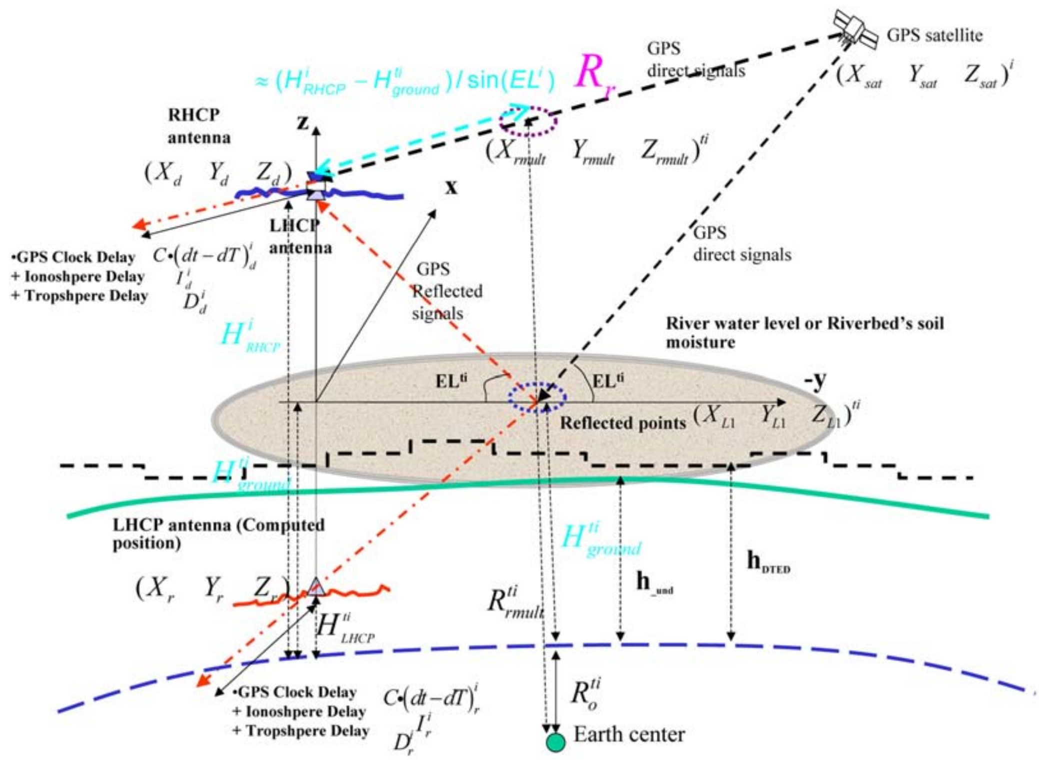

Fig 4

There are two ways of determining the height h_{DTED} at the RHCP receiver position for use in the ground height estimation. First, if the Digital Terrain Elevation Data (DTED level 2; ~30 M per pixel) is correct in an absolute sense, then a simple subtraction of the known DEM of the area from the DTED data is sufficient [2]. The altitude trial procedure repeats until the following condition is satisfied: $\left|H^{ti}_{ground} - h^{i}_{DTED}\right| \le 1.0\,\mathrm{m}$ [12]. An alternative is to use the satisfactory values of the relative heights. Second, the authors use the GPS data for H^{i}_{RHCP} and H^{ti}_{LHCP} for the subtraction as well as the DTED level 2 (~30 M per pixel) mapping of $h_{\_und}$. The value of $h_{\_und}$ is provided from the output of the GPS observations. Thus, the local ground or water surface altitude is described by (11).

$$H^{i}_{ground} = \frac{(H^{i}_{RHCP} + H^{i}_{LHCP})}{2} - h_{\_und} \qquad (11)$$

The standard deviation for the flood, river water level, or riverbed is given by (12).

$$\sigma^{i} = \left[\frac{\sum_{k=1}^{k=N}(H^{i}_{g} - \overline{H}_{g})^2}{(N-1)}\right]^{0.5} ; \quad \begin{array}{l} i : \text{ID of satellite} \\ g : \text{ground} \\ \overline{H}^{i}_{g} : \text{ mean of reflected height for i satellite} \\ N = \text{number of observed samples} \end{array} \qquad (12)$$

The surface roughness parameter (DISP) is defined as the ratio of the standard deviation of the surface height to the length of the reflected footprint. For low frequencies, the effect of roughness can be explained by the single roughness parameter DISP =(σ^{i} / L), where σ^{i}_{kg} is surface standard deviation and L is its horizontal correlation length, both expressed in wavelength units. the normalization of roughness parameter equation is conducted by [10] as given by (13).

$$\mathrm{DISP} = \frac{\text{standard deviation of } H_{ground}}{\text{length of reflected footprint}} \qquad (13)$$

$$= \frac{\sigma_{k=N,ground}}{\left((X_{k=N,L1} - X_{k=1,L1})^2 + (Y_{k=N,L1} - Y_{k=1,L1})^2 + (Z_{k=N,L1} - Z_{k=1,L1})^2\right)^{0.5}}$$

$(X_{k=1,L1} \quad Y_{k=1,L1} \quad Z_{k=1,L1})$: the initial position of Reflected point at K= 1 sample

$X_{k=N,L1} \quad Y_{k=N,L1} \quad Z_{k=N,L1})$: the initial position of Reflected point at K= N samples

Both methods yield similar results that compare well with the ground-based measurements of the ground height and stream water level. A comparison with independently measured elevation values is still not possible due to the residual multipath errors in the calculated height at the RHCP receiver positions.

2.3 Reflectivity and Ground Object Detection

The surface reflectivity $\Re$ can be used for the classification of ground objects. In [1], the resultant reflection coefficient is shown to be the sum of the co-polar and cross-polar reflection coefficients. Let Γ_0 and Γ_x be the co-polar and cross-polar reflection coefficients, respectively; the resultant reflection coefficient F_c is $F_c = \sqrt{\Gamma_0^2 + \Gamma_x^2}$. This coefficient is denoted as F_c and can be computed once the elevation angle is known; the coefficient has the form $F_c(EL)$, where EL is the elevation angle from the receiver to the satellite. $\Re$ is related to the reflection coefficient, power ratio between the reflected signal and the direct signal, and a correction factor due to soil moisture and soil content. More precisely, for Rough-surface at no-coherent signals, $\Re$ is expressed as

$$\Re = \frac{(\mathrm{SNR})_r - N_r}{(\mathrm{SNR})_d - N_d} \cdot F(EL, m_v, \mathrm{DISP}, \varepsilon') \quad (14)$$

Where $(\mathrm{SNR})_r$ and $(\mathrm{SNR})_d$ are the signal-to-noise ratios of the reflected and direct signals, respectively. The two terms N_r and N_d represent the noise levels along the reflected and direct paths, respectively; these terms also depend on the LHCP and RHCP antennas and channels. The correction factor $F(EL, m_v, \mathrm{DISP}, \varepsilon')$ is used to model the soil roughness DISP , soil moisture m_v , dielectric constant of soil or water ε' . Let l be the emissivity of the soil moisture and ε' be the dielectric constant of the soil or water, it is known that [10] the two terms are related by the relation $l = 1 - \left|\frac{1-\sqrt{\varepsilon'}}{1+\sqrt{\varepsilon'}}\right|^2$. The dielectric constant ε' , however, is a function of m_v and the composition of the reflecting surface, which is characterized in terms of the sand and clay contents as the percentage of the dry weight of soil. The reflectivity at rough surface and soil moisture results are presented by Chang & Blagoy [11]. The dielectric constant ε' is assumed to be a function of soil moisture m_v , percentage of sand $\%\mathrm{sand}$, and percentage of clay $\%\mathrm{clay}$ of the following as:

$$\begin{aligned} \varepsilon' &= \left(a_0 + a_1(\%\mathrm{sand}) + a_2(\%\mathrm{clay})\right) \\ &+ m_v\left(b_0 + b_1(\%\mathrm{sand}) + b_2(\%\mathrm{clay})\right) \qquad (15) \\ &+ m_v^2\left(c_0 + c_1(\%\mathrm{sand}) + c_2(\%\mathrm{clay})\right) \end{aligned}$$

In the above, a_0 , a_1 , a_2 , b_0 , b_1 , b_2 , c_0 , c_1 , and c_2 are coefficients that are given as follows:

$$a_0 = 2.75,\ a_1 = 0.71,\ a_2 = 0.55$$
$$b_0 = 0.37,\ b_1 = -1.5,\ b_2 = -2.5$$
$$c_0 = 45.0,\ c_1 = 135.0,\ c_2 = 115.0$$

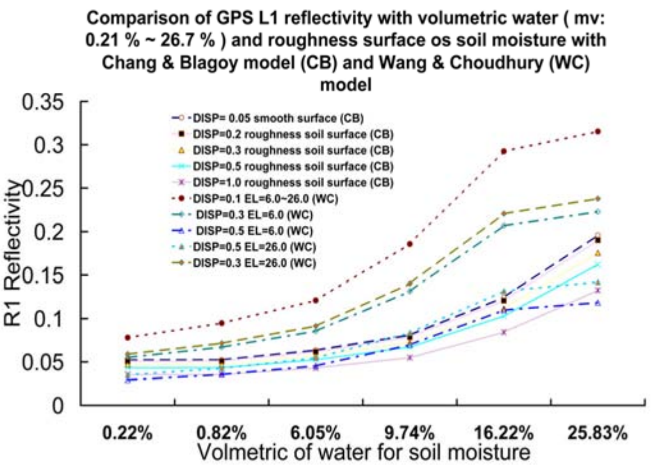

Fig 5

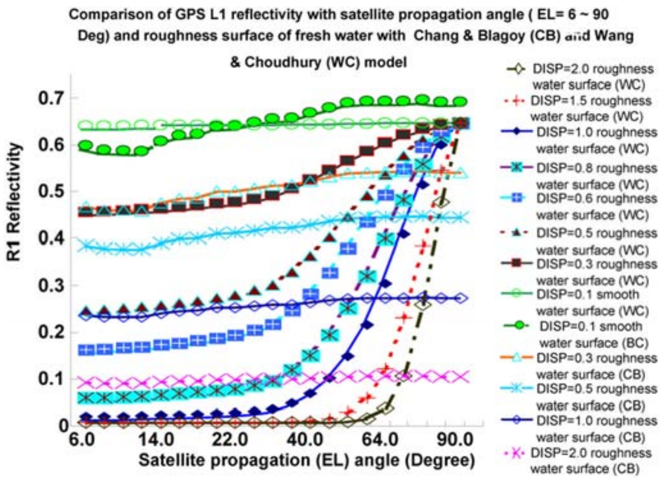

Fig 6

The soil sample is textually a sand loam soil, with a composition within the topsoil of 51.5 % sand, 10.3 % clay, 38.2 % silt. Further, the correction factor for the water surface of a river $F(\mathrm{DISP},\varepsilon') \cong F(EL, m_V, \mathrm{DISP}, \varepsilon')$ can be expressed and simplified as [12]

$$F(\mathrm{DISP},\varepsilon') = \frac{1-l}{\exp(\mathrm{DISP})} \qquad (16)$$

For the evaluation of emissivity, a semiempirical expression proposed by Wang and Choudhury [13], which includes the effect of roughness, has been introduced as [14]

$$l = 1-((1-Q)\Re_H - Q\Re_V)\exp(-4k^2\sigma^2\cos^2(EL))$$

where $\Re_H$ and $\Re_V$ are the smooth-surface reflectivities for the H and V polarizations, respectively. Q is a mixing polarization parameter that depends on the operating frequency and σ ; k is the wave number in free space, including those analyzed in this paper. for smooth-surface, $\Re$ is expressed as

$$\Re = (1-Q)\Re_H + Q\Re_V = \frac{1-l}{\exp(4k^2\sigma^2\cos^2(EL))} \qquad (17)$$

Fig. 5 depicts a comparison of reflectivity vs. soil moisture and surface roughness for sand loam soil measurements with Chang & Blagoy and Wang & Choudhury model. It is further remarked that during the processing of the reflected GPS signals, several parameters can be simultaneously obtained. As a result, for each satellite, the local height h_{ground} , roughness DISP^i, and reflectivity $\Re^i_j$ can be obtained. The superscript i is used hereafter to denote a relevant term with respect to the i -th satellite. In addition, the term may be a function of the frequency as well. Hereafter, the subscript j is used to denote the frequency. Fig. 6 depicts a comparison of reflectivity vs. fresh water and surface roughness measurements with Chang & Blagoy and Wang & Choudhury model.

The correction factors obtained from [11] for the five values of DISP ($\mathrm{DISP} = 0.041 \sim 1.0$), Small values of DISP ($DISP \le 0.1$) correspond to smooth surfaces. The $\Re$ should be expressed by Eq. (14) for no-coherent signals and [13] for coherent signals. However, right after tillage a value of $DISP = 0.5$ is possible. Large values of DISP ($DISP \ge 0.51$) correspond to rough surfaces. The $\Re$ should only be expressed by eq. (14) for no-coherent signals. ε' ($\varepsilon' = 3 \sim 81$), and l ($l = 0.36 \sim 0.928$) are shown in Table I. From these values, it is observed that ε' = 81 for the river water and ε' = 3~13 for the bare soil at the riverside and the soil moisture on the riverbed.

In Table I, the normalization DISP is derived by s.t.d of surface heights when s.t.d of the surfaces are rough.

TABLE I. Correction factors for rough surfaces

ε'	DISP / l	$F(\mathrm{DISP},\varepsilon') = (1-l)/\exp(\mathrm{DISP})$				
		0.041	0.073	0.114	0.514	1.0
3 mv:0.1 %	0.928	0.069	0.067	0.064	0.043	0.026
5 mv:2.2 %	0.854	0.140	0.136	0.130	0.087	0.054
10 mv: 15 %	0.730	0.259	0.251	0.241	0.161	0.099
13 mv:26%	0.682	0.386	0.374	0.359	0.241	0.148
30	0.522	0.459	0.444	0.426	0.286	0.176
40	0.472	0.507	0.491	0.472	0.316	0.194
72 (Sea)	0.377	0.598	0.579	0.556	0.372	0.229
81 (River)	0.36	0.614	0.595	0.571	0.383	0.235

III. MEASUREMENTS AND RESULTS

In this section, the results of field experiments will be presented.

3.1 Reflected Point Results

The measure and altimetry elevation for river, riverbed, and ground object classification throughout the reflected GPS signals at different location was described. So that the reflected area of river, riverside (bare soil), and riverbed (soil moisture) on Lan-Yang Bridge on Lan-Yang river, Yi-Lan was made and described (UTC Time 2007 07 13 02 43 17-02 58 44 UT (10:43- 10:58 am LT)) (was showed as Fig. 7) with the results.

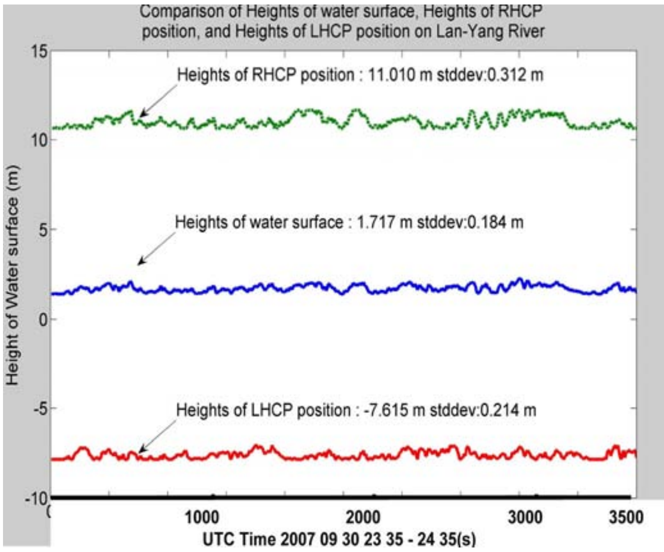

Fig 7

The water levels on a sunny day (2007/09/30) are determined and described by using the results of the RHCP/LHCP receiver positions for software simulation and measurement process region (shown in Fig. 8). The stream water level is $1.717\,m \pm 0.184\,m$ on a sunny day (2007/09/30) in Lan-Yang River, Yi Lan, Taiwan. A couple of standard deviation from $11.012\,m \pm 0.312\,m$ height of RHCP and $-7.612\,m \pm 0.214\,m$ height of LHCP conducted

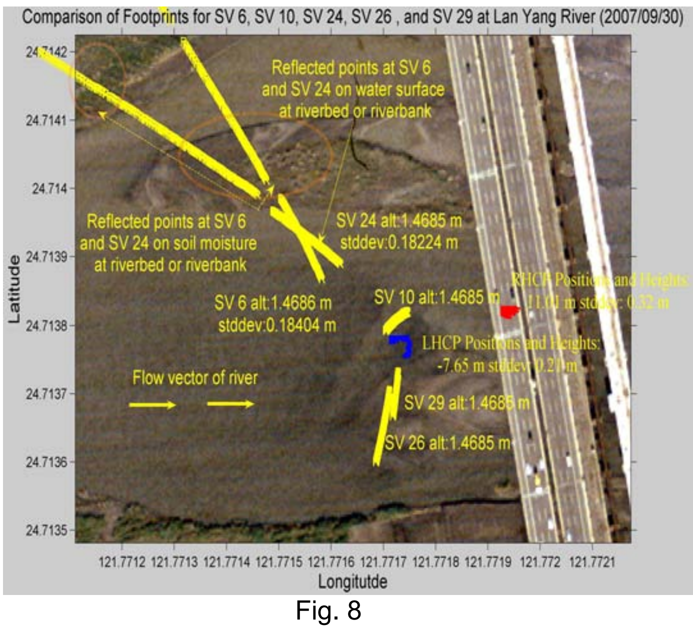

Fig. 8

and reduced (85%) to the standard deviation of height for water surface.

3.2 Signal Analysis Results

Fig. 9. predicts that the standard deviation (0.184 m) for a river water level $\bar{h}_{ground}$ of $1.717\,\mathrm{m}$ is less than the standard deviations (0.312 and 0.214 m, respectively) for an RHCP antenna height $\bar{h}_{RHCP}$ of $11.012\,\mathrm{m}$ and LHCP antenna height $\bar{h}_{LHCP}$ of $-7.612\,\mathrm{m}$ because the accuracy of the river surface height depends on the heights of the RHCP (like a base station) and LHCP (like a rover) antennas.

Fig. 9. shows comparisons of the reflectivity on a sunny day (2007/09/30) at the Lan-Yang River, Yi Lan, Taiwan. Fig. 9. predicts the reflectivity, propagation (EL) angle, and SNR for PRN 6 and PRN 24. The differences between reflectivities R1 for PRN 6 are in the range 0.01~0.57 on the propagation angle $EL^6 = 6.5^o \sim 22.5^o$ of PRN 6, $\mathrm{DISP}^6 = {0.18}/{76.9} = 0.0024$ and $F(\mathrm{DISP})_{water} = 0.638$. The differences between reflectivities R1 for PRN 24 amount to 0.001~0.46 on the propagation angle $EL^{24} = 6.5^o \sim 25.0^o$ of PRN

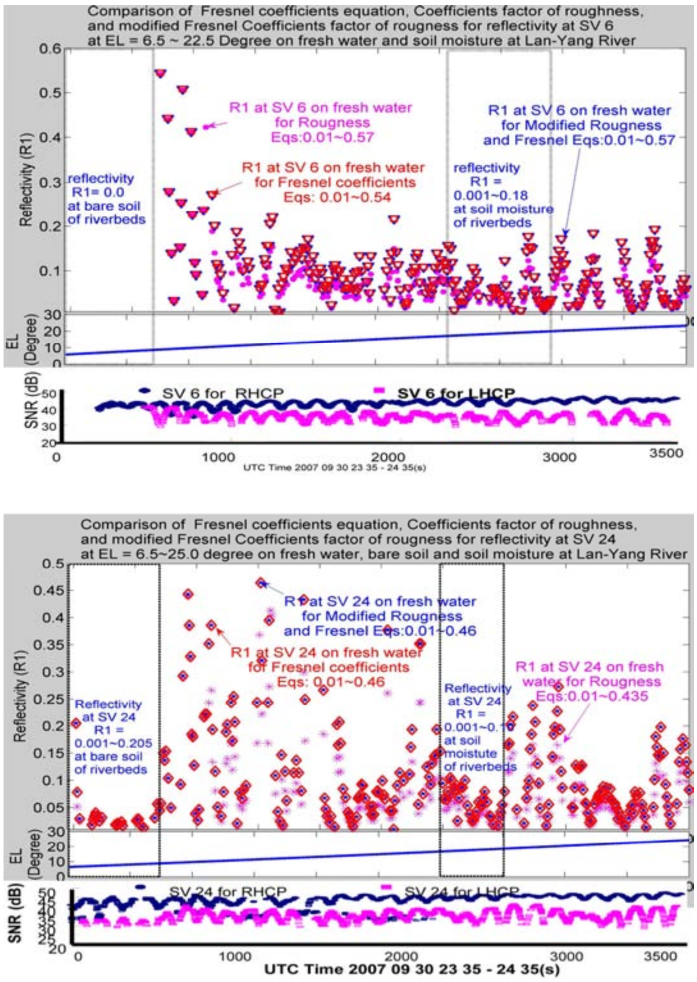

Fig. 9

24, $\mathrm{DISP}^{24} = 0.18/67.6 = 0.0027$ and $F(\mathrm{DISP})_{water} = 0.638$. Moreover, the signals reflected from the river soil moisture surface for PRN 24 have a two time period of 500 s (during time: 0 ~ 500 s) with R1 for PRN 24 decay to 0.001~0.205 on the propagation angle $EL^{24} = 6.5^{o} \sim 10.0^{o}$ of PRN 24, ($\mathrm{DISP}^{29} = 0.18/7.29 = 0.025$) is almost like that of a smooth surface. The differences between reflectivities R1 $\mathrm{DISP}^{24} = 0.185/22.5 = 0.0087$, and $F(\mathrm{DISP})_{\mathrm{bare\_soil}} = 0.269$ and 350 s (during time: 2250 ~ 2600 s) with R1 for PRN 24 decay to 0.001~0.102 on the propagation angle $EL^{24} = 16.5^{o} \sim 20.0^{o}$ of PRN 24, °, $\mathrm{DISP}^{24} = 0.192/62.57 = 0.0028$ and $F(\mathrm{DISP})_{\mathrm{wet\_soil}} = 0.478$; (see PRN 24 reflected footprint of Fig. 8).

The receiver continues to track and lock on the reflected signals for PRN 6 on riverside and riverbank. The soil moisture surface for PRN 6 have a one time period of 560 s (during time: 2350 ~ 2910 s). Because the R1 for PRN 6 decay to 0.01~0.18 on the propagation angle $EL^{6} = 17.5^{o} \sim 21.5^{o}$ of PRN 6 , $\mathrm{DISP}^{6} = 0.185/72.3 = 0.0025$ and $F(\mathrm{DISP})_{\mathrm{wet\_soil}} = 0.478$ (see PRN 6 reflected footprint of Fig. 8).

The signals reflected from the river water surface for PRN 10, PRN 26 and PRN 29. (see PRN 10, PRN 26 and PRN 29 reflected footprint of Fig. 8) Fig. 10. predicts the reflectivity on river surface, propagation (EL) angle, and SNR for PRN 10, PRN 26 and PRN 29. The length of the reflected footprint for PRN 29 is 7.29 m and the standard deviation of altitude σ^{29}_{ground} for PRN 29 is 0.18 m. The roughness of water surface for the PRN 29 The differences between reflectivities R1 for PRN 29 on river surface are in the range 0.01~0.19 at $F(\mathrm{DISP})_{water} = 0.626$ on the propagation angle $EL^{29} = 42.0^{o} \sim 72.0^{o}$ of PRN 29.

The length of the reflected footprint for PRN 26 is 11.92 m and the standard deviation of σ^{26}_{ground} for PRN 26 is 0.182 m. The roughness of water surface for the PRN 26 reflection point ($\mathrm{DISP}^{26} = 0.182/11.92 = 0.0154$) is almost like that of a smooth surface. The differences between reflectivities R1 for PRN 26 on river surface are in the range 0.01~0.57 at $F(\mathrm{DISP})_{water} = 0.633$ on the propagation angle $EL^{26} = 26.5^{o} \sim 54.8^{o}$ of PRN 26,.

The differences between reflectivities R1 for PRN 10 on river surface are in the range 0.01~0.43 at $\mathrm{DISP}^{10} = 0.18/5.25 = 0.035$ and $F(\mathrm{DISP})_{water} = 0.626$ on the propagation angle $EL^{10} = 57.2^{o} \sim 50.9^{o}$ of PRN 10,.

Authors make accurate qualitative measurements with calibration procedure for the RHCP and LHCP receivers and antennas. The

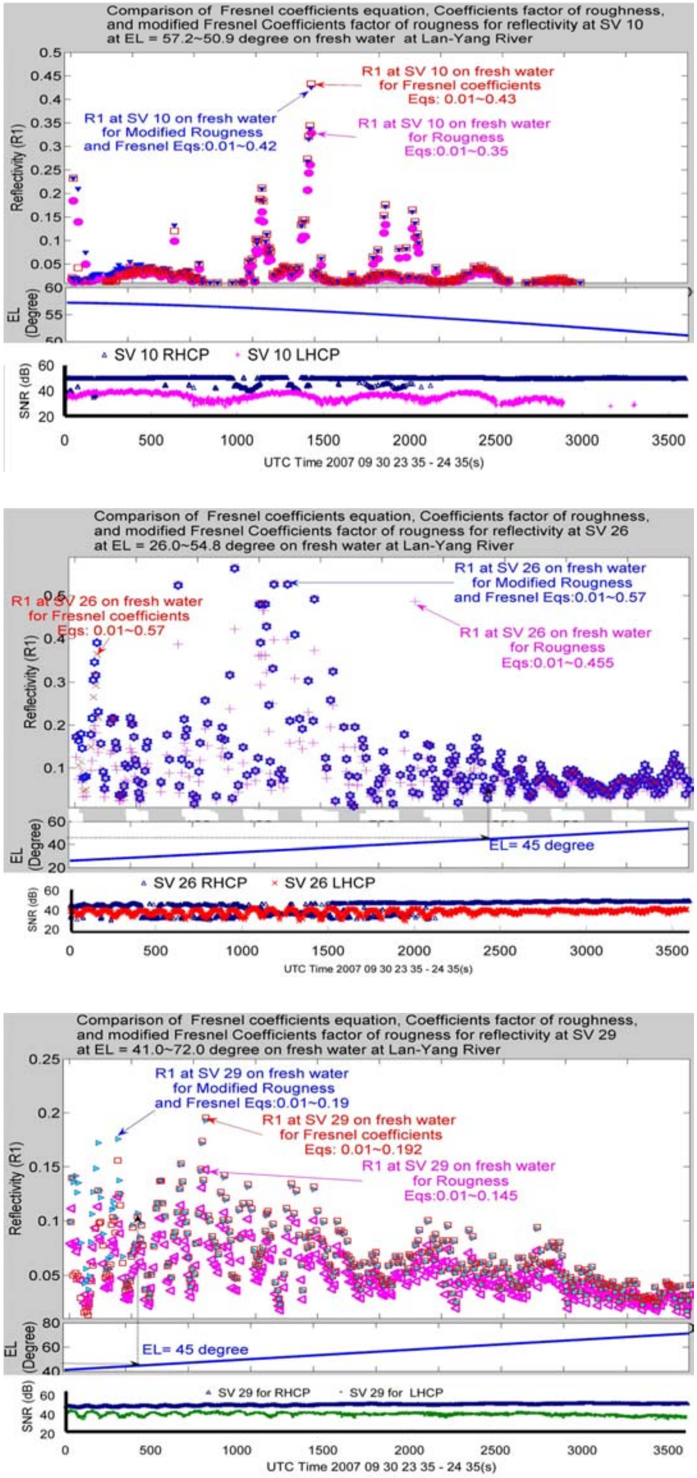

Fig. 10

correlation time of this signals process is about 3600 sec. Fig. 11. predicts that the average of time to obtain a stable results is 45 sec at normalization surface roughness parameter $\mathrm{DISP} \leq 0.1$ for PRN 6 and PRN 24 on the propagation angle $EL^{i} = 6.5^{o} \sim 25.0^{o}$. The average of time to obtain a stable results is 650 sec at normalization surface roughness parameter $\mathrm{DISP} \leq 0.1$ for PRN 10, PRN 26 and PRN 29 on the propagation angle $EL^i = 25.0^o \sim 72.0^o$. All these issues are important for understanding of GPS signal scattering and retrievals of either surface heights or soil moisture.

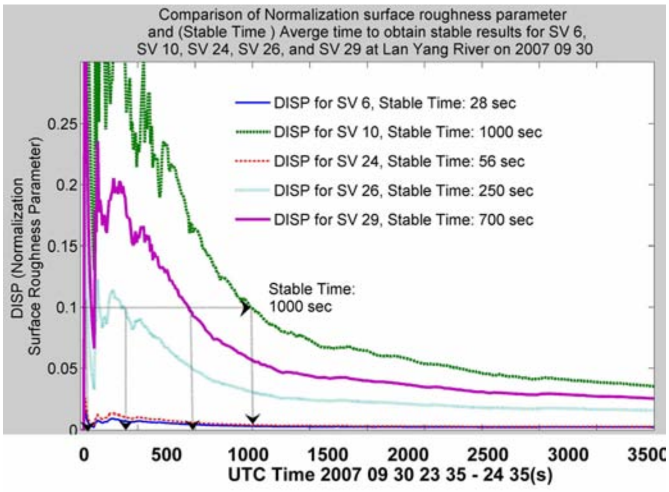

Fig. 11

3.2 Soil Moisture Results

In the following, the reflectivity and soil moisture results are presented based on the analysis of experiments. Fig. 12 depicts a comparison of reflectivity vs. soil moisture and surface roughness for measurements at Lan-Yang River (PRN 6). The reflectivity from stream soil moisture with roughess surface $\Re_1^6 = 0.05 \sim 0.205$ and volumetric water (m_v : 0.82 % ~ 12.0 %) of soil moisture is as similar as reflectivity with Wang Choudhury model at DISP=0.3~0.5 on the propagation angle $EL^i = 6.0^o \sim 26.0^o$. Further, the reflectivity from stream soil moisture with smooth surface $\Re_1^6 = 0.02 \sim 0.05$ and volumetric water (m_v : 0.22 % ~ 1.0 %) of soil moisture is as similar as reflectivity with Chang & Blagoy model at DISP=0.1~0.5 on the propagation angle $EL^i = 6.0^o \sim 26.0^o$.

Fig. 13 depicts a comparison of reflectivity vs. soil moisture and surface roughness for measurements at Lan-Yang River (PRN 24). The reflectivity from stream soil moisture with roughness surface $\Re_1^{24} = 0.05 \sim 0.10$ and volumetric water (m_v : 0.82 % ~ 8.5 %) of soil moisture is as similar as reflectivity with Wang Choudhury model at DISP=0.3~0.5 on the propagation angle $EL^i = 6.0^o \sim 26.0^o$. Further, the reflectivity from bare soil on riverside with roughness surface $\Re_1^6 = 0.01 \sim 0.07$ and volumetric water (m_v : 0.1 % ~ 0.4 %) of soil moisture is as similar as reflectivity with Chang & Blagoy model at DISP=0.1~1.0 on the propagation angle $EL^i = 6.0^o \sim 26.0^o$.

The reflectivity of soil moisture is between 0.02 and 0.205 for stream soil moisture and bare soil with roughness surface $\text{DISP}^i = 0.01 \sim 1.0$ and volumetric water (m_v : 0.1 % ~ 12.0 %) in sandy-loam soil moisture at GPS L1 band.

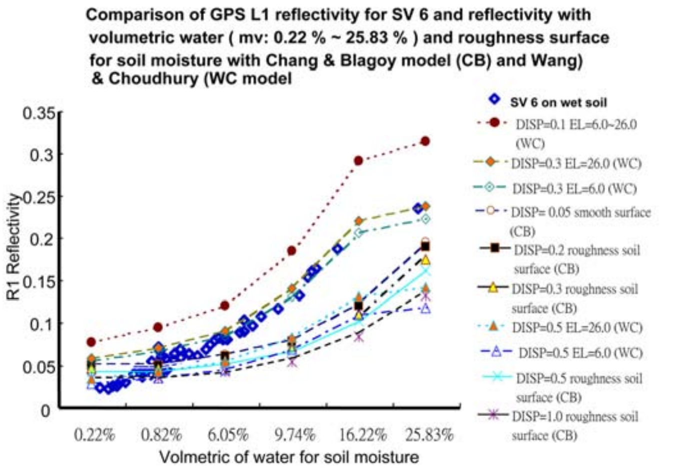

Fig. 12

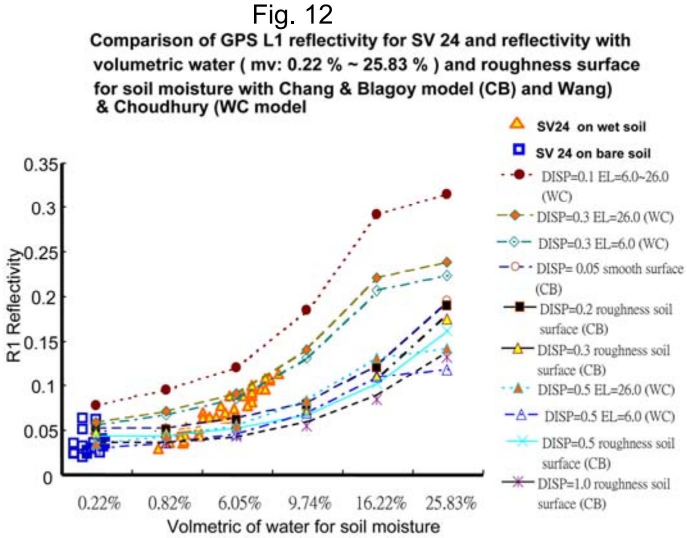

Fig. 13

3.3 Roughness surface water and propagation angle Results

Fig. 14 depicts a comparison of reflectivity vs. low propagation angle ($EL^i = 6.5^o \sim 25.0^o$) and surface roughness water for measurements at Lan-Yang River (PRN 6 and PRN 24). The reflectivity from stream water with roughness surface $\Re_1^i = 0.02 \sim 0.23$ is as similar as reflectivity with Wang Choudhury model at DISP=0.3~1.0 on the propagation angle $EL^i = 6.0^o \sim 26.0^o$. Further, the reflectivity from stream water with roughness surface $\Re_1^6 = 0.23 \sim 0.57$ is as similar as reflectivity with Chang & Blagoy model at DISP=0.1~1.0 on the propagation angle $EL^i = 6.0^o \sim 26.0^o$.

Fig. 15 depicts a comparison of reflectivity vs. other propagation angle ($EL^i = 25.0^o \sim 72.0^o$) and surface roughness water for measurements at Lan-Yang River (PRN 10, PRN 26, and PRN 29). The reflectivity from stream water with roughness surface $\Re_1^i = 0.01 \sim 0.25$ is as similar as reflectivity with Wang Choudhury model at DISP=0.6~1.0 on the propagation angle $EL^i = 25.0^o \sim 60.0^o$. The reflectivity from stream water with roughness surface $\Re_1^i = 0.25 \sim 0.62$ is as similar as reflectivity with Chang & Blagoy model at DISP=0.1~1.0 on the propagation angle $EL^i = 25.0^o \sim 60.0^o$. Further, the reflectivity from stream water with roughness surface $\Re_1^i \leq 0.1$ for PRN 10 and PRN 29 is as similar as the reflectivity with Wang & Choudhury model at DISP=1.0~2.0 on the propagation angle $EL^i = 60.0^o \sim 72.0^o$.

In these measurements, the reflectivity of stream water is between 0.01 and 0.62 for fresh water with roughness surface $\mathrm{DISP}^i = 0.1 \sim 2.0$ on propagation angle $EL^i = 6.0^o \sim 72.0^o$ at GPS L1 band.

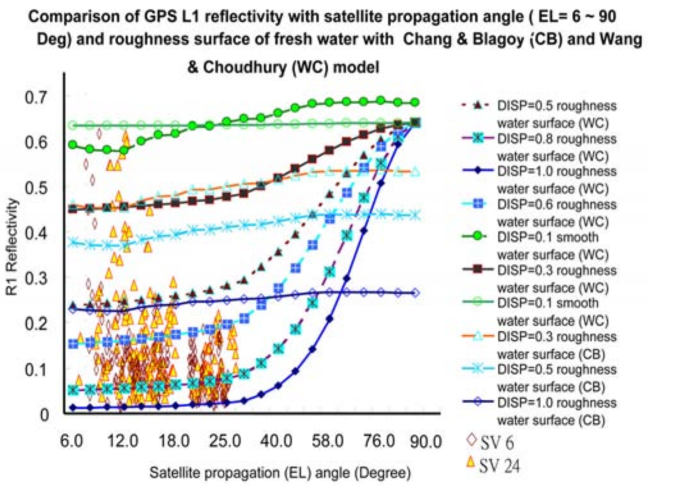

Fig. 14

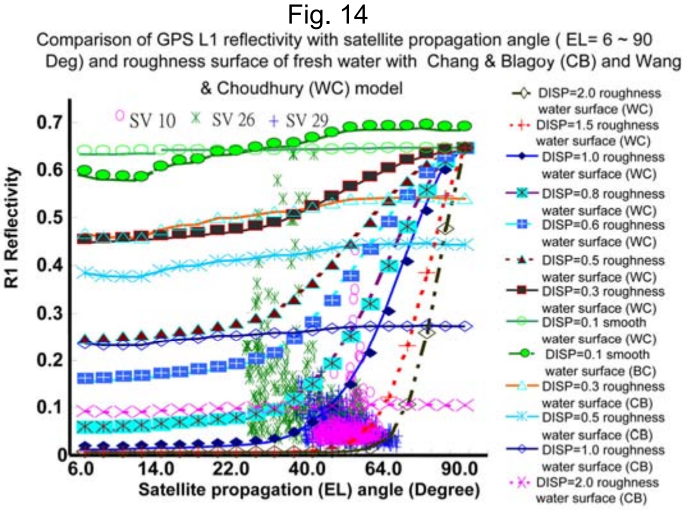

Fig. 15

IV. SUMMARY AND CONCLUSION

The results of this study demonstrate the usefulness of the GPS reflectivity estimation model in estimating the reflectivities of the river water, riverside, riverbank, and riverbed rapidly and with a high accuracy. This paper presents the results of reflectivity simulations. The study has shown that the accuracy performance of the developed algorithms is robust with respect to the GPS L1/L2 signature distributions for the river water, riverbank, and riverside. This algorithm can be used for obtaining the reflectance spectra by monitoring the flood level in storm weather. It is found that the monitoring of stream levels was improved (standard deviation = 0.18 m) by approximately 45~50% by using the correlated with the existing model of DTED altitude database and the correction of undulation height. The soil moisture classification accuracy is improved by approximately 75~80% by using correction factor $F(EL, m_v, \mathrm{DISP}, \varepsilon')$ and multispectral (reflectivity) data along with normalization surface roughness parameters. The use of GPS for determining the values $\Re_1^i = 0.01 \sim 0.62$ for the river water, riverbed, and riverside provides a low-cost, high-resolution, and more accurate method as compared to other soil moisture measurements such as airplane and ground-based measurements. This paper can guarantee optimum performance in monitoring high accuracy flood water level, soil moisture of riverbed and bare soil of riverside.

Acknowledgment

The authors would like to thank Mr. C. H. Chen for his help with the GPS observations during storm weather. The authors also thank Dr. Wickert and Dr. Georg Beyerle for their suggestions and assistance with the instantaneous ionospheric delay and tropospheric delay effects in real-time weather data and for sharing their research method during the author's visit to GFZ, Berlin, in 2007.

REFERENCES

[1] D. Manandhar, R. Shibasaki, H. Torioto, "Prototype software-based receiver for remote sensing using reflected GPS signals," *ION Proceedings,* Page(s): 643 – 652, *GNSS*, 2006.

[2] J. P. Weiss, P. Axelrad, S. Anderson, "Assessment of digital terrain models for multipath prediction at geodetic GNSS installations," *ION Proceedings,* Page(s): 2815 - 2823*, GNSS*, 2006.

[3] M. S. Grant, S. T. Acton, S. J. Katzberg, "Terrain moisture classification using GPS surface-reflected signals," *IEEE Geoscience and Remote Sensing Letters*, vol. *4*, no. *1*, 41-45, January, 2007.

[4] L. C. Shen, J. C. Juang, C. L. Tseng, C. L. Tsai, C. C. Chang, "New application of reflected GPS signals L1/L2 observation techniques with an integrated GPS receiver for remote measurements and digital terrain elevation mapping," *IEEE Instrumentation and Measurement Technology Conference* IMTC 2007

1–3 May 2007, pp. *1–6*, 10.1109 / IMTC .2007.379233.

[5] L. C. Shen, J. C. Juang, C. L. Tseng, C. L. Tsai, "Remote sensing stream flow discharge and soil classification by using reflected GPS observations, L1 and L2 reflectivity and digital terrain model," *ION Proceedings,* Page(s): 1643 – 1650, *GNSS*, 2007.

[6] S. T. Lowe, C. Zuffada, Y. Chao, P. Kroger, J. L. LaBrecque, L. E. Young, "Five-cm-precision ion aircraft ocean altimetry using GPS reflections," *Geophysical Research Letters*, vol. *29*, no. *10*, May, 2002.

[7] C. C. Goad and K. Borre, *RECPOS Least-squares Searching for Receiver Position for MATLAB*. MATLAB Software Supply. 19 April, 1996.

[8] P. Joosten, *Integer Ambiguity Estimation Using LAMBDA (Basic Version) for MATLAB*. MATLAB Software Supply. 19 May, 1999. Mathematical Geodesy and Positioning Delft University of Technology. Ch. 1-ch. 4, pp. 15-45

[9] P. J. G. Teunissen, P. J. De Jonge, C. C. J. M. Tiberius, The least-squares ambiguity decorrelation adjustment: Its performance on short GPS baselines and short observation spans, *Journal of Geodesy*, vol. *71*, no. *10*, pp. *589–602*, 1997.

[10] J. Behari, *Microwave Dielectric Behavior of Wet Soil*. New Delhi, India: Anamaya, ch. 1,2, pp. *7–38*, 2005.

[11] Z. Y. Chang, P. Blagoy, J. Frank, C. Gerard, "Extending the limits of a capacitive soil-water-content measurement," *IEEE Transactions on Instrumentation and Measurement*, vol. *56*, no. *6*, ,2240-2244, December, 2007.

[12] L. C. Shen, J. C. Juang, C. L. Tsai, "Remote sensing coastal sea level and ocean tide by using reflected GPS L1 and L2 observation for integrated GPS receiver," *IEEE/MTS Proceedings*, Kobe, Japan, OTO 2008.

[13] J. R. Wang and B. J. Choudhury, "Passive microwave radiation from soil: Examples of emission model and observations, "in Passive Microwave Re-mote Sensing of Land–Atmosphere Interactions. Zeist, The Netherlands: VSP, 1995.

[14] Claudia Notarnicola, Mariella Angiulli, and Francesco Posa "Soil Moisture Retrieval From Remotely Sensed Data: Neural Network Approach Versus Bayesian Method", IEEE TRANSACTIONS ON GEOSCIENCE AND REMOTE SENSING, VOL.46, NO.2, pp. *547–557* 2008

Lie Chung Shen received the B.S. from Aeronautical Engineering department, Chung Cheng Science and Institute University, Lon-Tan, Taiwan in 1983, M.S. degree from the department of Mechanic Engineering, National Central University, Chung-Li, Taiwan in 1990, He is a PhD candidate at Earth research and academy, National Chung Kung University, Taiwan.

Jyh-Ching Juang received the B. S. and M. S. degrees from National Chiao-Tung University, Hsin-Chu, Taiwan, in 1980 and 1982, respectively, and the Ph. D. degree in electrical engineering from University of Southern California, Los Angeles, in 1987. He was with Lockheed Aeronautical System Company, Burbank before he joined the faculty of the Department of Electrical Engineering, National Cheng Kung University, Tainan, Taiwan in 1993. His research interests include sensor networks, GNSS signal processing, and software-based receivers.

Chia-Chyang Chang received the BSc and MSc degrees from Chung Cheng Institute of Technology (CCIT) and National Cheng Kung University (NCKU), respectively, both in Taiwan. He received a PhD degree in space geodesy from the University of Nottingham (UK) in 1995. He was a full professor at the Department of Surveying and Mapping Engineering, CCIT, and the Department of Information Management, Yuda University, before he joined the Department of Applied Geomatics, Ching Yun University, all in Taiwan, in 2007. His research interests include satellite navigation, geodetic monitoring, mobile positioning, and location-based services.